DOI:
10.1016/j.bbamcr.2021.119024

Document Version
Peer reviewed version

Live cell ATR-FTIR spectroscopy as a novel bioanalytical tool for cell glucose metabolism research.

Anchisa Poonprasartporn and K.L. Andrew Chan*

Institute of Pharmaceutical Science, School of Cancer and Pharmaceutical Sciences, King's College London, SE1 9NH, United Kingdom

**e-mail: ka_lung.chan@kcl.ac.uk*

1. Introduction

Diabetes remains one of the leading causes of death globally with 4 million deaths reported in 2019 and it is predicted that it will be the 7th leading cause of death worldwide in 2030. It was estimated that more than 400 million were living with diabetes to date and it could be risen to 700 million in 2045. Around 20% of the elderly (>65 years old) have diabetes and 374 million people are at increased risk of developing type 2 diabetes. Moreover, it was estimated that half of people with diabetes are underdiagnosed (1-3). Diabetes is a major cause for both micro and macro vascular complications such as retinopathy, nephropathy, atherosclerosis and peripheral artery disease, which can worsen the patients' quality of life. The global annual cost of treatment and the disease and its complications management was 825 billion dollars in 2014, with the largest cost to individual countries being in China ($170 billion), the USA ($105 billion) and India ($73 billion), respectively (5).

Powerful analytical methods for the development of highly effective and safe medications for diabetic treatment is highly important. Cell-based biochemistry with metabolite measurement is a key platform of diabetes and metabolism research. Metabolomics is currently a promising method that can identify and quantify metabolites from biological samples. Low molecular weight molecules such as lipids, amino acids, peptides, nucleic acids, and carbohydrates, have important roles in disease/metabolism studies, and therefore rich metabolome data are highly valuable. However, dynamics in biological rhythm and interference from non-specific substances are some of the challenges that can affect the analysis outcome (7, 8). Non-destructive methods for metabolomics measurement of live cell, which is often preferred over measuring dead, lysed cell, for drug/cell metabolism is still lacking. Techniques that have been reported for studying metabolites in live cells includes colorimetric assays, fluorometric assays and immunoassays. However, due to the complex metabolic changes in cells, multiple assays are often needed to increase the specificity, which made these approaches expensive, laborious and time-consuming.

Fourier-Transform Infrared (FTIR) spectroscopy is a non-destructive, non-invasive, label-free, chemically specific and high-throughput technique. FTIR analysis of cells have been shown to be able to distinguish the different stages of cell cycle (9) , cell death (10) drug-cell sensitivity and resistance (11, 12) diseases (13) and biomedical changes from the clinical biomarkers in various type of cancers (14-17). FTIR has been introduced in diabetes and metabolism research since 2007 as a diagnostic tool for the analysis of chemical deposition in hair samples with different blood sugar levels (18). In 2013, FTIR has been shown to be able to clearly differentiate healthy and type I diabetic rats (19) and diagnose diabetes in human from the measurement of blood, urine, lip and saliva (20-23). FTIR also represents a promising blood-glucose monitoring tool during insulin and metformin treatment (18, 24). Interestingly, FTIR spectroscopy can be used to diagnose diabetes with and without retinopathy complication from patients' blood sample with 90% sensitivity, 92.7% specificity, and 90.5% overall accuracy (25). However, metabolism in live cells, which has the potential to improve the understanding of diabetes, has not yet been demonstrated. We hypothesize that live-cell FTIR can produce useful biomolecular information that can aid diabetes research. The aim of this work is to demonstrate that live-cell FTIR can be used to study the chemical transformation of hepatocyte from

the healthy state (cultivated in normal glucose level) to diabetic state (after exposed in hyperglycaemia condition for 24 hr) (26-28) to relate and confirm the metabolism change in cells.

2. Materials and Methods:

Human hepatocyte carcinoma cell (HepG2) were kindly provided by Professor Khuloud Al-Jamal (School of Cancer and pharmaceutical science, King's College London). Cells were maintained in Dulbecco's Modified Eagle's Medium (DMEM from Sigma Aldrich, UK) high glucose containing 10% fetal bovine serum (FBS from Sigma Aldrich, UK), 50 U/mL penicillin and 100 µg/mL streptomycin, 1% non-essential amino acid and 1% L-glutamine. Cells were maintained in T25 culture flask and incubated in a humid atmosphere containing 5% CO_2 at 37°C.

2.1 Cell viability assay

Cells were tested with a ranging concentration of glucose-supplemented DMEM CO_2 independent medium (Sigma Aldrich, UK) to ensure the cell remain viable at the concentration used in the live-cell FTIR experiment. The number of living cells were detected based on the 3-(4,5-dimethylthiazol-2-yl)-2,5-diphenyltetrazolium bromide (MTT) assay. Cells concentration of $2.0x10^4$/200 µL were cultured in 96-well plates for 24 hours and treated with the different concentrations of glucose (5, 10, 25, 35, 50, 75 and 100 mM). Cells were cultured with each concentration for 24, 48 and 72 hours, and then 100 µL of the MTT reagent (0.5mg/mL) (VWR International) was added to each well. After 2 hours of incubation, 100 µL of DMSO was added to each well to detect the presence of formazan. The absorbance value at 570 nm was taken using a spectrophotometer (SpectraMAX™ software). The values of absorbance of each well plate were plotted and the percentage cell viability were calculated over each individual concentration compared with control by Microsoft Excel program.

2.2 Live-cell FTIR measurement

HepG2 cells in the T25 flask were trypsinised at ~80% confluence and suspended with $2x10^6$/2 mL in DMEM CO_2 independent medium. The cells were seeded on the temperature-controlled ZnS attenuated total reflectance (ATR) plate with 10 reflections on the sampling side (HATR, Pike Technologies, USA; ZnS ATR crystal was purchased from Crystran Ltd., UK). The plate was sealed with a warmed lid to avoid evaporation. This condition also let the attached cell to reach high confluence on the ATR element's measuring surface as shown in Figure 1. According to the small penetration depth of measurement, around 2-3 µm from the ATR element's surface (smaller than the thickness of the living cell (~5-10 µm), absorbances are contributed mainly from the attached live cells with negligible contribution from the medium (11, 29-31).

Visible images of cells on the ZnS ATR plate and in T25 flask were respectively captured in reflection and transmission mode after 24 hours of incubation using a 10x objective. The seeded HepG2 cell spectra were monitored for 24, 48 and 72 hours using a FTIR spectrometer (Tensor II, Bruker Optics). Normal glucose (3.8 mM; control) or high glucose (25 mM) concentrations in DMEM CO_2 independent medium was applied for the cell-glucose metabolism study. After seeding the cells in the live-cell ATR plate, a measurement was taken every 10 minutes at 8 cm^{-1} spectral resolution with 9 minutes scanning time (1024 scans) for a total duration of 24 hours. DMEM CO_2 independent medium was used to avoid the requirement of 5% CO_2 at the spectrometer.

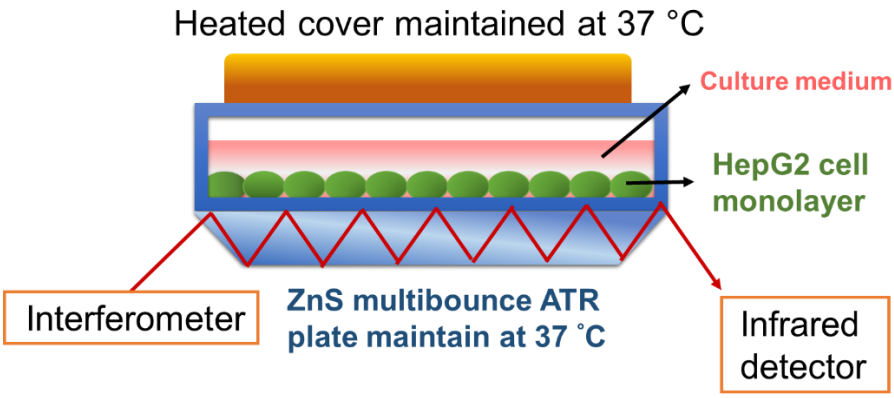

Figure 1. A schematic diagram showing the live cell ATR-FTIR experiment set up [Single column fitting]

The cell suspension was incubated for 24 hours to allow cell attachment. Once cells were attached, which is indicated by a slow but steady growth in the amide II band (around 24 hour), the medium was changed to fresh normal glucose (3.8 mM in 2% FBS DMEM CO_2 independent medium; control) or high glucose (25 mM in 2% FBS DMEM CO_2 independent medium; diabetic) medium. A background was measured at this point. The change of spectrum was then monitored for a further 72 hours with a measurement taken at every 10 minutes. Each experiment was repeated for 3 times based on 3 independent cultures with a similar passage number range 24-34 and on a different day.

2.3 Data processing and analysis

Spectra were water vapor compensated and cut to the wavenumber range of 1780-900 cm^{-1}, followed by concave rubber band baseline correction (1 iteration with 16 baseline points was found to be sufficient) and vector normalisation. Principal component analysis (PCA) from PyChem® software (available from :http://pychem.sourceforge.net/) was used as the statistical tool for possibly correlated changes observation from the experiment setting (32). T-test was applied to find the significant difference among the treatment groups compared to control. Significance difference was defined as *P.value* < 0.05 calculated using Microsoft Excel.

3. Results

3.1 Cell culturing

To established that the HepG2 cell behaviour is similar between cells cultured under standard protocols and under experimental conditions, i.e. on the ZnS ATR plate, visible images of HepG2 cells captured 24 hours after seeding on the ATR plate in the DMEM CO_2 independent medium have shown that cells were fully attached (Figure 2A). Comparing to cells cultured in T25 tissue culture flask incubated with standard DMEM medium in 5% CO_2 environment, the cells have shown a similar morphology (Figure 2B). Selected spectra of a typical experiment of the living cells, with culture medium as the background, are shown in Figure 3A. The cells have shown a small absorbance 2 hours after seeding, which rapidly increased at the 4^{th} hour. The seeded cells had further grown on the ATR plate for another 20 hours until the increase in absorbance had clearly plateaued, which is an indication of a full attachment of cell layer on the ATR plate (33-35). The spectra of HepG2 cell have shown clear peaks of amide I at 1645 cm^{-1}, amide II at 1550 cm^{-1}, $\nu_{sym}(COO^-)$ at 1400 cm^{-1}, amide III at 1235 cm^{-1}, the asymmetric and symmetric stretching mode of phosphate bands between at ~1240 and

1080 cm^{-1} and the carbohydrates bands between 1150-1000 cm^{-1} (Figure 3A.). Figure 3B shows the averaged spectra measured from the three separate repeated experiments of live HepG2 cells at the 24^{th} hour after seeding, the very small standard deviations (grey colour) represented the high reproducibility of the ATR FTIR experiments.

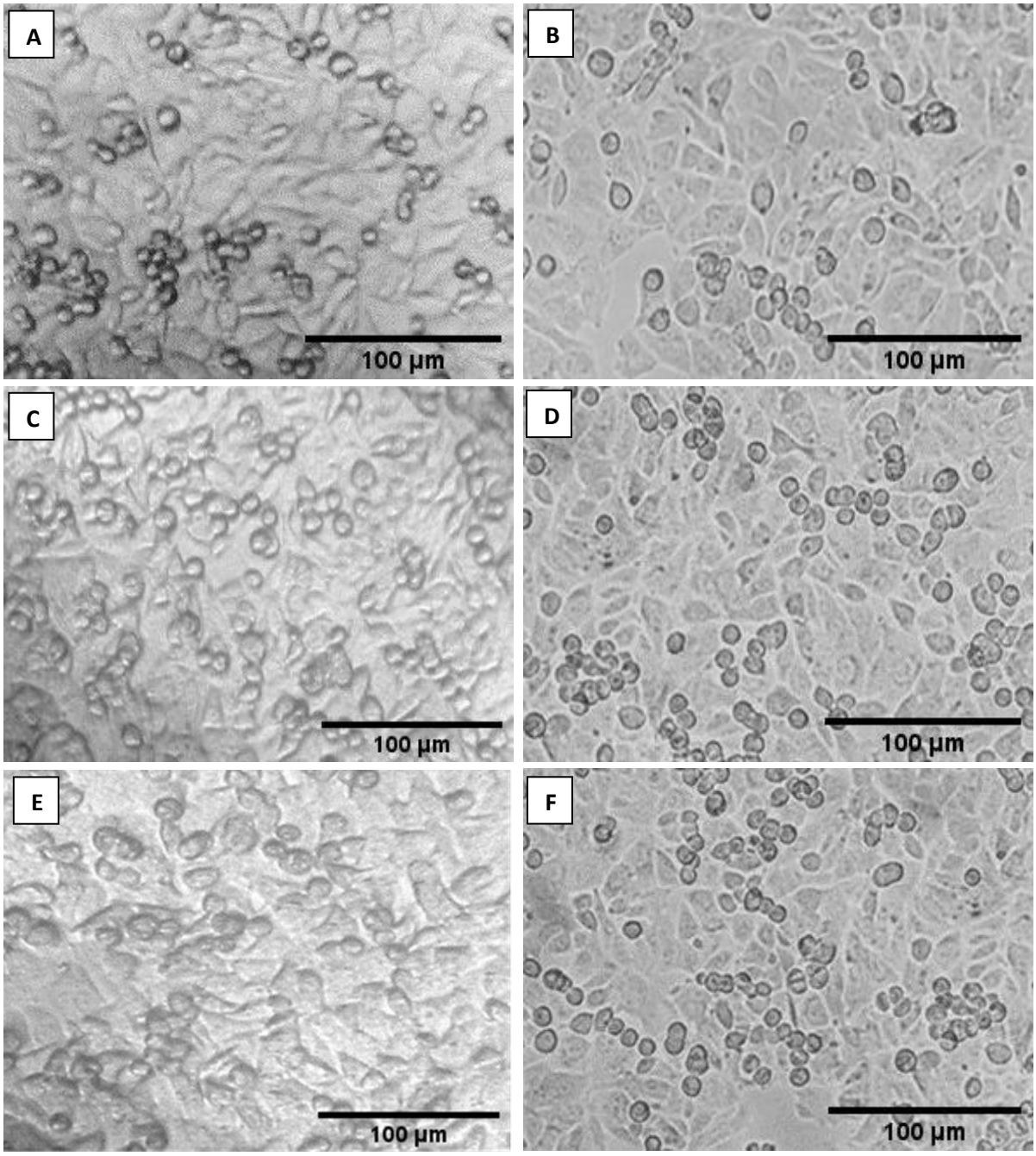

Figure 2. Image of HepG2 cells at different time of seeding on the ATR element and T25 flask, respectively; 24 hour A and B, 48 hour C and D, 72 hour E and F [double column fitting]

When the cells reached the plateau phase, around 24 hours after seeding, the medium was replaced by the test medium to the attached cells for the study of the reaction between cells and the testing conditions.

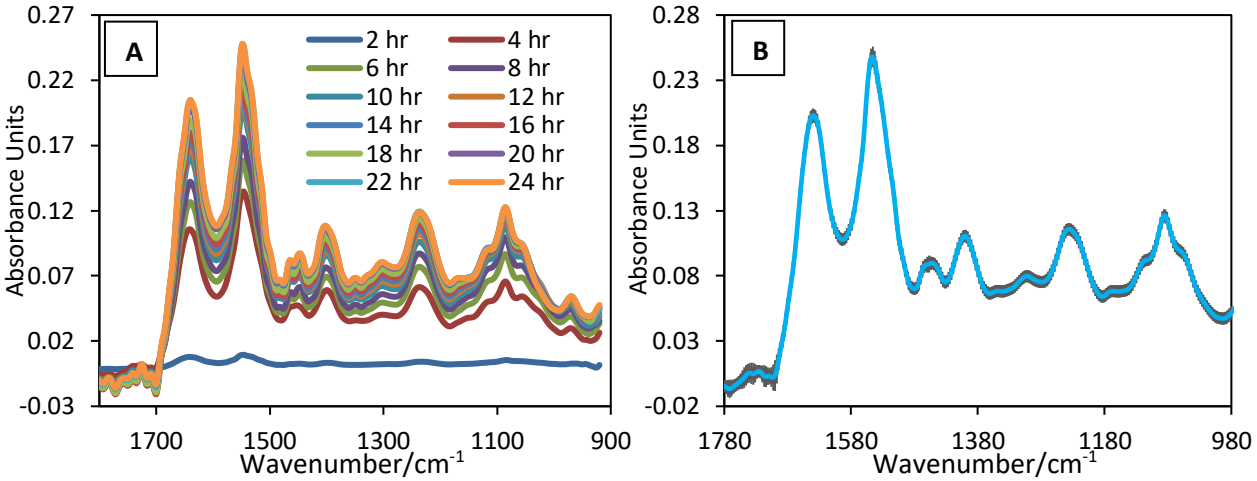

Figure 3. HepG2 FTIR live cell spectra every 2hr of seeding time (A) and the error bars of 24th hour (B) [double column fitting]

To further confirm that the ATR substrate and the CO_2 independent medium produces a cell behaviour that is comparable to other diabetic studies in the literature using the HepG2 cell model, we have compared the viability of cells according to the published IC50 of glucose for HepG2 cells, which was ~50 mM at 72 h in diabetes studies (36). The results have shown that >80% of the HepG2 cell had survived in 5 and 10mM with insignificance differences when compared to control. At 50 mM and 72-hour incubation, the cell viability has dropped to 50% (Figure. 4), which is similar to the results from the literature ($p<0.05$ compared to normal glucose treatment) (37).

In this experiment, 25 mM was selected for the high glucose concentration because it is commonly used to create diabetic cell models (26, 36-38). Figure 4 shows that there is insignificant effect on the viability of cells at the 25 mM glucose treatment compared to control for all duration of treatments. Our previous studies (33-35) on anticancer agent has shown that cell-death can produce significant changes to the cellular molecular composition, the results in Figure 4 shows that cells remain largely viable at 25 mM and therefore confirming that cell death is not a signification contributor to the differences between high glucose (25 mM) and control (normal glucose) treatments. This ensures that the difference observed between high and normal glucose treated cells are due to a change in metabolism of cells rather than cell death.

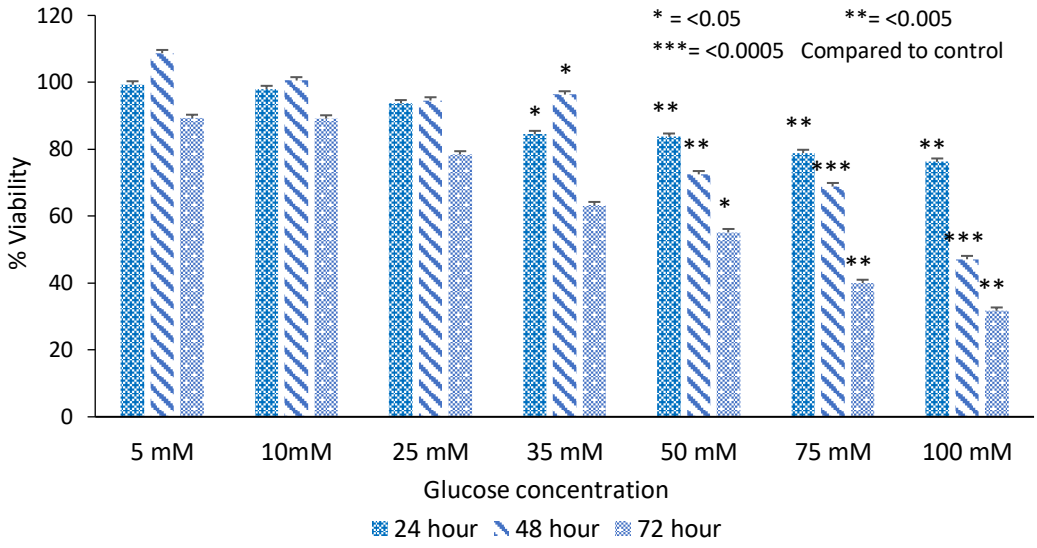

Figure 4. HepG2 cell viability compared to control (3.8mM) for 24, 48 and 72 hours [1.5 column fitting]

3.2 Live cell FTIR experiment

Figure 5A shows the representative spectra of HepG2 cells treated in medium with 25mM glucose (hyperglycaemia model) measured at 3 different time points (24, 48 and 72 hour) with the spectral range between 3800-800 cm^{-1}. The spectra were obtained using the first measurement after the change of medium as the background to highlight the spectral changes as a result of the change of medium. High spectral noise occurred in the 3600-3000 and 900-800 cm^{-1} regions due to the strong aqueous water absorption and are excluded in the analysis. The three representative spectral have shown major changes in the fingerprint region between 1700-900 cm^{-1} as highlighted in Figure 5B. Cells appeared to have continued to grow slowly 24 hours after the medium change with an increase in the amide II band (a key marker for protein) but slightly reduced towards the 72nd hour, which is in agreement with the MTT assay results. Clear changes in the phosphate and carbohydrate bands in the 1350-950 cm^{-1} are apparent and the changes are consistent across the three repeated experiment. Figures 6 shows all spectra from the repeated measurements after 24- 48- and 72-hour treatments with a marked difference can be observed between the normal and 25 mM glucose treatment groups. Pair-wised PCA of the normal glucose versus 25 mM glucose treatment in this range has reviewed a clear grouping with PC1 showing statistical difference of <0.025, <0.01 and <0.03 for 24th, 48th and 72nd hour, respectively. The normal glucose treated cells has seen an increase in the absorbance at 1088, 1240 and 1400 cm^{-1} (Figure. 6B). These spectral peaks are associated with phosphate nucleic acid stretching mode PO^{2-} and symmetric stretching of COO^{-} which is from fatty acids, amino acids and carboxylate metabolites vibration. Whereas the high glucose treated cells at 24th hour have shown a clear reduction of the PO^{2-} stretching mode band. At time 48th and 72nd, an increasing band at ~1200 cm^{-1} is shown.

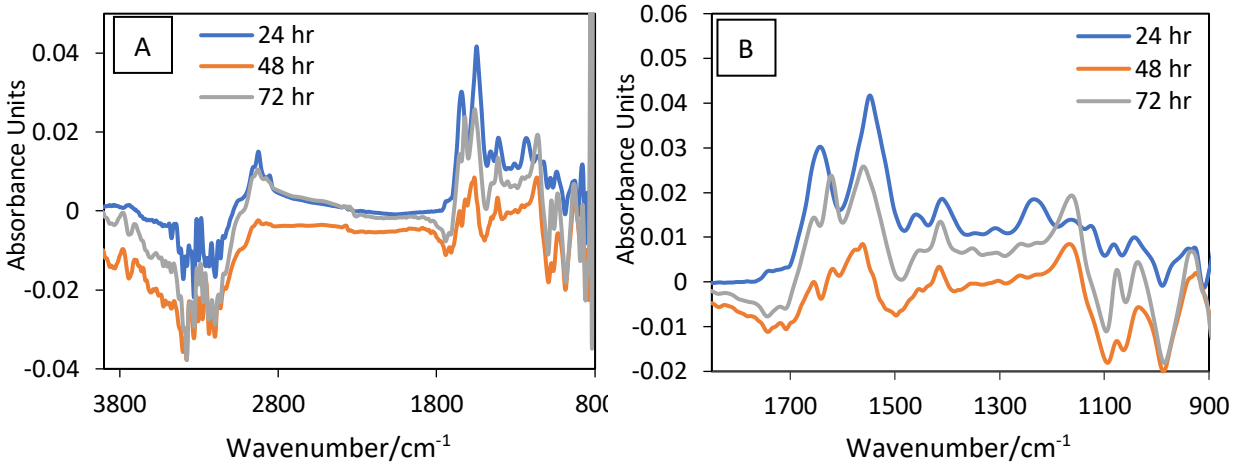

Figure 5. Spectra of HepG2 treated with 25mM glucose in 3 different time points (24, 48 and 72 hour) with spectra range between 3800-800 cm^{-1} (A) and spectra range between 1780-900 cm^{-1}(B) [double column fitting]

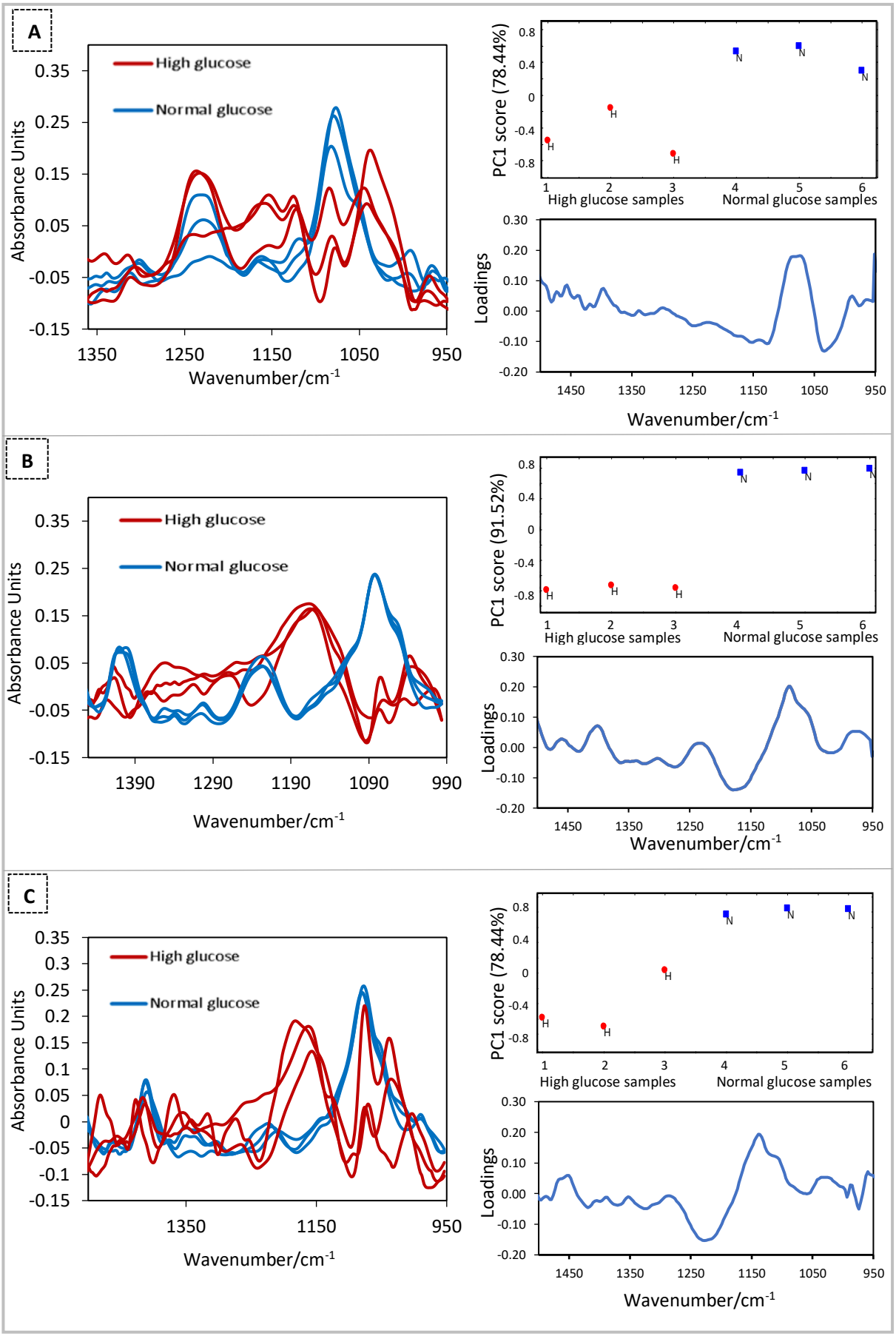
A
High glucose
Normal glucose
Absorbance Units
0.35
0.25
0.15
0.05
-0.05
-0.15
1350
1250
1150
1050
950
Wavenumber/cm-1
PC1 score (78.44%)
0.8
0.4
0
-0.4
-0.8
1
2
3
4
5
6
High glucose samples
Normal glucose samples
H
N
Loadings
0.30
0.20
0.10
0.00
-0.10
-0.20
1450
1350
1250
1150
1050
950
Wavenumber/cm-1
B
High glucose
Normal glucose
Absorbance Units
0.35
0.25
0.15
0.05
-0.05
-0.15
1390
1290
1190
1090
990
Wavenumber/cm-1
PC1 score (91.52%)
0.8
0.4
0
-0.4
-0.8
1
2
3
4
5
6
High glucose samples
Normal glucose samples
H
N
Loadings
0.30
0.20
0.10
0.00
-0.10
-0.20
1450
1350
1250
1150
1050
950
Wavenumber/cm-1
C
High glucose
Normal glucose
Absorbance Units
0.35
0.3
0.25
0.2
0.15
0.1
0.05
0
-0.05
-0.1
-0.15
1350
1150
950
Wavenumber/cm-1
PC1 score (78.44%)
0.8
0.4
0
-0.4
-0.8
1
2
3
4
5
6
High glucose samples
Normal glucose samples
H
N
Loadings
0.30
0.20
0.10
0.00
-0.10
-0.20
1450
1350
1250
1150
1050
950
Wavenumber/cm-1

Figure 6. The spectral changes as a function of time (left panel) between HepG2 treated in high (Red) and normal (Blue) glucose solution and the corresponding PCA1 score and loading plots (right panel) at (A) 24th, (B) 48th and (C) 72nd hour. [double column fitting]

4. Discussion

An adequate energy supply for the vital organs in the body is regulated by glucose homeostasis. Liver has an essential role in controlling several pathways of glucose metabolism including glycolysis, gluconeogenesis, glycogenesis, and glycogenolysis (39, 40).

During the feeding stage, glucose molecules from the carbohydrate digestion process enter the hepatocytes where they are phosphorylated to glucose 6-phosphate followed by several metabolic pathways to generate adenosine triphosphate or ATP. The catabolism of glucose into pyruvate, in term of glycolysis, is conserved as a crucial pathway to produce ATP. Pyruvate is carried into the mitochondrial matrix where it is transformed to acetyl-CoA by pyruvate dehydrogenase cascading enzyme and integrated into the tricarboxylic acid cycle (TCA) in concurrence with oxaloacetate. The TCA cycle generates the electron carriers for electron transport chain-oxidative phosphorylation, to produce ATP in the final process. The extra amount of carbohydrates in the liver are converted into glycogen and stored as the energy reserve in the liver and muscle cells (glycogenesis). Moreover, in high carbohydrate diet, the excess amount of dietary glucose is also converted into lipid (lipogenesis) and stored in the adipose tissue. Liver glucose homeostasis during fasting stage is also crucial. When blood sugar level drops, liver releases glucose to the bloodstream either from the stored glycogen(glycogenolysis) or by breaking down triglyceride to glycerol and combined with alanine and lactate to produce glucose(gluconeogenesis)(40, 41).

Glucose-cell metabolism imbalance can induce the metabolic syndromes such as insulin resistance type 2 diabetes, obesity, non-alcoholic fatty liver disease (NAFLD), and cardiovascular conditions. Several *in vivo* studies have demonstrated that oxidative stress, inflammation, and disease progression are due to glucotoxicity (42-46). However, complex alterations such as endocrines, hormones and environmental factors may influence the physiological metabolite change in the energy metabolism and organ responses (47, 48). Thus, in vitro study may be an ideal platform to better understand glucose metabolic change inside cells.

Immortal hepatocyte cell lines are widely used to explain the regulation of hepatic metabolism. The primary hepatocyte cells are better than the cancerous cell line because they mimic more the *in vivo* situation. But the primary hepatocyte availability and accessibility are limited. Moreover, the phenotype is unsteady, and this cell type can only be culture for a short period (49, 50). Sefried et al. (29) have demonstrated and compared the gluconeogenesis gene expression and protein regulated hepatic metabolism or hepatokine among primary hepatocyte and immortalized cell lines; AML12, THLE-2, and HepG2. The results showed that HepG2 cells appear to be closer to the *in vivo* situation than AML12, THLE-2 despite its tumorigenic origin. Thus, we concluded that regarding the similarity of HepG2 cell line hepatic gene expression, this cancerous cell line can be used in *in vitro* of the diabetes-related research.

.

Live-cell FTIR measurements show cellular changes overtime in normal glucose treatment are mainly from the growth of the seeded cells. The symmetric and asymmetric phosphate stretching mode at 1078 cm^{-1} and 1220 cm^{-1} regions, which are originated from DNA backbone and phospholipids products from cell expansion, have continued to rise as a function of incubation time. Another two major regions that indicates cell expansion are Amide III (1220 cm^{-1}), which is overlapped with the asymmetric phosphate band, and the amide II band at 1550 cm^{-1}. These two bands have shown simultaneously increasing with the phosphate peaks. Increases in these spectral regions have confirmed the cells were growing in the normal glucose treatment (Figure 7).

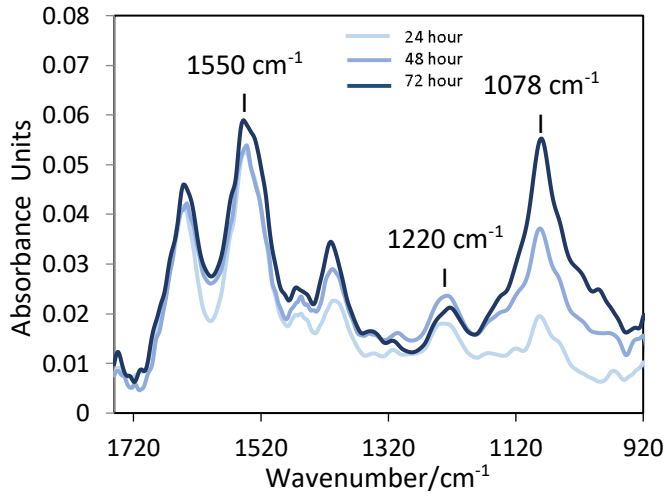

Figure 7. Comparison of normal glucose treated HepG2 FTIR spectra for time 24th 48th and 72nd hour [Single column fitting]

On the other hand, normalized FTIR cells spectra treated in high (25 mM) glucose have revealed a different pattern of cellular component changes when compared to the normal treatment. Clear different changes are found in the phosphate stretching and carbohydrate spectral band regions, which has shown an overall decrease in absorbance overtime (Figure. 8) relative to the protein amide II peak, suggesting large changes in the phosphate and carbohydrates metabolites in the cells upon high glucose treatment.

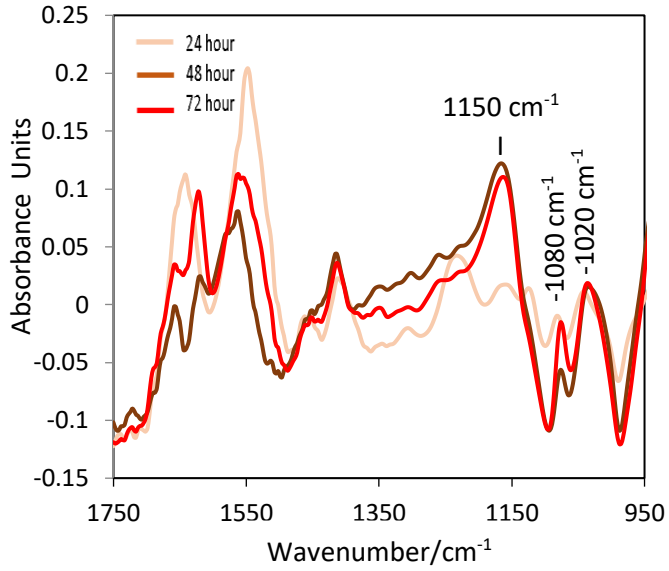

Figure 8. Comparison of high glucose treated HepG2 normalized FTIR spectra for time 24th 48th and 72nd hour [Single column fitting]

According to the literature of hepatic glucose utilization, hepatocytes consume glucose as a fuel to produce ATP from ADP through oxidative phosphorylation. Excess glucose would be converted into glycogen and store in the liver. Comparison of the spectral changes of the HepG2 cells exposed in high glucose for 24 h to the difference spectra of ATP-ADP has shown a remarkable similarities as shown in Figure 9, suggesting the production of ATP from the phosphorylation of ADP can be observed using live cell FTIR measurement. Furthermore, a closer look at the spectral change at 48th and 72nd hour exposure, a rise in the characteristic glycogen peaks at ~1020, 1080 and 1150 cm$^{-1.}$ (51)(Figure 8) can be observed, indicating that FTIR can detect the glucose metabolism changes in the treated cells.

Energy metabolism in the normal cell culture condition depends mainly on the oxidative phosphorylation (OXPHOS) for ATP production because ATP, which is the key energy unit, is more efficiently produced from this process (36 ATP) than glycolysis (2 ATP)(49). However, many types of cancer cells prefer using the glycolytic pathway due to a permanent impairment of mitochondrial OXPHOS, as founded by Otto Warburg (50). However, this view is altered by recent publications which found that the function of mitochondrial OXPHOS in most cancers is still intact. Cancerous cells have different metabolic phenotypes of energy metabolism even in the same type of origin. Due to the common trait of rapid growth, they adapt and reprogram to the environmental change to overcome disturbance of growth conditions. Therefore, the ratio between glycolysis and OXPHOS to yield total ATP is flexible for cancer cells, which results in a selective advantage over non-cancerous cell in unfavourable environments (49).

ATP is the determinator of cellular mitochondrial respiration. The amount of intracellular ATP is subtly changed by metabolic inhibitor in order to test mitochondrial toxicity. The level of ATP is generally sustained in normal living cell. While cells became injured, the intracellular ATP amount can be lowered rapidly. Thus, an advanced technique for ATP extraction, which is normally analysed from lysed/fixed cell, that avoid cell degradation from both physical and nonphysical procedures is essential (52). Rita et al. (53) have developed and verified a one-step extraction and bioluminescence assay for quantifying glucose and ATP levels in cultured HepG2 cells in high glucose condition for testing drug-induced mitochondrial toxicity. The advantage of this method over traditional biochemical assay is that it requires only one extraction step that disintegrate cellular proteins with concomitants and release steadily of cellular glucose and ATP from HepG2 cells. The method allows the measurement

of considerable changes in ATP levels with no detectable cell loss (no protein content disruption) suggesting that the proposed assays could be a precise multiparameter-based measurement of the effects of cytoprotective/cytotoxic compounds. However, the limitation of this method compared to the parallel cytometry assay is, it cannot distinguish between live and dead cells, where the glucose contents and ATP are not comparable.

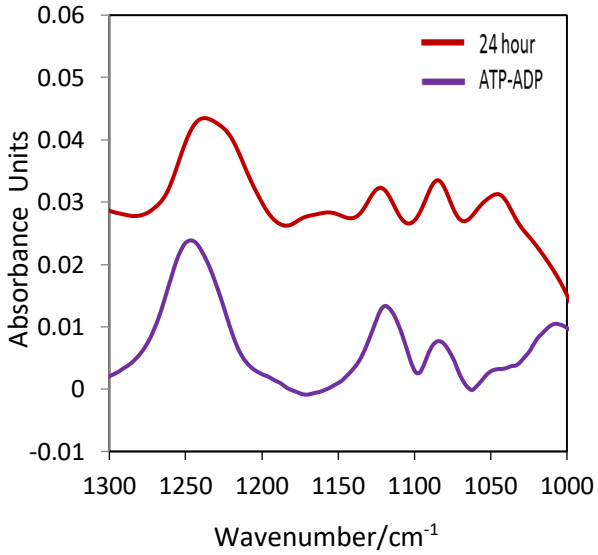

Figure 9. Comparison between ATP-ADP FTIR spectrum and high glucose treated HepG2 at time 24th [Single column fitting]

Whilst the conversion of ADP to ATP and glycogen in cells can be measured using conventional biochemical essays or LC/MS metabolomics approach, we would like to highlight the outstanding benefits of the live-cell FTIR method, such as it can continuously automatically measuring the cells throughout the experiment, the method does not require any labelling and there is no need to destroy or extract the metabolites from the cell samples. There are no expensive chemical reagents required and the measurement is relatively quick. Although the measurement was set to scan for 9 min per spectrum in this experiment as the timescale for the cellular changes was relatively slow in this case, high quality spectra can typically be obtained in less than a minute.

5. Conclusions

In conclusion, live-cell FTIR helps to understand diabetes and can be an additional tool for providing some information that can assist in the study of diabetes. In the future, live-cell FTIR can be applied to study glucose-cell metabolism related to other organs e.g. pancreas, muscle, and adipose cell or potentially be an alternative tool for drug-cell metabolism study.

6. Acknowledgements

We thank Prof Khuloud Al-Jamal's research group for helps and advice on cell culturing. We thank Dr Andrei Tarasov from Oxford for the stimulating discussion. We thank Dr Ali Altharawi for general support. We also thank the Thai Government for providing a PhD studentship for Anchisa Poonprasartporn to carry out this research. We also thank EPSRC (EP/L013045/1) for the funding that started this research theme in the group.

7. References

1. Moneta GL. Diabetes mellitus, fasting blood glucose concentration, and risk of vascular disease: a collaborative meta-analysis of 102 prospective studies. Yearbook of Vascular Surgery. 2011;2011:49-51.
2. Bourne R, Stevens G, White R, Smith J, Flaxman S, Price H, et al. Causes of vision loss worldwide, 1990-2010: A systematic analysis. The Lancet Global Health. 2013;1.
3. Saeedi P, Petersohn I, Salpea P, Malanda B, Karuranga S, Unwin N, et al. Global and regional diabetes prevalence estimates for 2019 and projections for 2030 and 2045: Results from the International Diabetes Federation Diabetes Atlas, 9th edition. Diabetes Research and Clinical Practice. 2019;157:107843.
5. Zhou B, Lu Y, Hajifathalian K, Bentham J, Di Cesare M, Danaei G, et al. Worldwide trends in diabetes since 1980: a pooled analysis of 751 population-based studies with 4·4 million participants. The Lancet. 2016;387(10027):1513-30.
7. Gonzalez FJ. Challenges and Opportunities of Metabolomics. Journal of cellular physiology. 2018;227(8):2975-81.
8. Zhang A SH, Wang P, Han Y, Wang X. Modern analytical techniques in metabolomics analysis. Analyst. 2012;2012 Jan 21;137(2):293-300.
9. Holman HY MM, Blakely EA, Bjornstad K, McKinney WR. IR spectroscopic characteristics of cell cycle and cell death probed by synchrotron radiation-based Fourier transform IR spectromicroscopy. Biopolymers (Biospectroscopy) 2000;57:329-35.
10. Kuimova M, Chan KLA, Kazarian S. Chemical Imaging of Live Cancer Cells in the Natural Aqueous Environment. Applied spectroscopy. 2009;63:164-71.
11. Falé P, Altharawi A, Chan KLA. In situ Fourier transform infrared analysis of live cells response to doxorubicin. Biochimica et biophysica acta. 2015;1853.
12. Rutter AV SM, Filik J, Sandt C, Dumas P, Cinque G, Sockalingum GD, Yang Y, Sulé-Suso J. Study of gemcitabine-sensitive/resistant cancer cells by cell cloning and synchrotron FTIR microspectroscopy. Cytometry A. 2014;2014 Aug;85(8):688-97.
13. Roy S, Perez-Guaita D, Andrew DW, Richards JS, McNaughton D, Heraud P, et al. Simultaneous ATR-FTIR Based Determination of Malaria Parasitemia, Glucose and Urea in Whole Blood Dried onto a Glass Slide. Analytical Chemistry. 2017;89(10):5238-45.
14. Frederick W, Koehler V, Eunah L, Kidder LH, Lewis EN. Near infrared spectroscopy: the practical chemical imaging solution. Spectros Eur. 2002 June/July:12-9.
15. Liu K-Z, Jia L, Kelsey SM, Newland AC, Mantsch HH. Quantitative determination of apoptosis on leukemia cells by infrared spectroscopy. Apoptosis. 2001;6(4):269-78.
16. Kumar S, Shabi TS, Goormaghtigh E. A FTIR Imaging Characterization of Fibroblasts Stimulated by Various Breast Cancer Cell Lines. PLOS ONE. 2014;9(11):e111137.
17. Harvey T, Henderson A, Gazi E, Clarke N, Brown M, Faria E, et al. Discrimination of prostate cancer cells by reflection mode FTIR photoacoustic spectroscopy. Analyst. 2007;132:292-5.
18. Sundaramoorthi K, Sethu G, Ethirajulu S, Raja Marthandam P. Efficacy of metformin in human single hair fibre by ATR-FTIR spectroscopy coupled with statistical analysis. J Pharm Biomed Anal. 2017;136:10-3.
19. Severcan F, Bozkurt O, Gurbanov R, GÖRgÜLÜ G. FT-IR spectroscopy in diagnosis of diabetes in rat animal model. Journal of biophotonics. 2010;3:621-31.
20. Eikje N. Diabetic interstitial glucose in the skin tissue by atr-ftir spectroscopy versus capillary blood glucose. Journal of Innovative Optical Health Sciences. 2010;03.
21. Yang X, Fang T, Li Y, Guo L, Li F, Huang F, et al. Pre-diabetes diagnosis based on ATR-FTIR spectroscopy combined with CART and XGBoots. Optik. 2019;180:189-98.
22. Yoshida S, Yoshida M, Yamamoto M, Takeda J. Optical screening of diabetes mellitus using non-invasive Fourier-transform infrared spectroscopy technique for human lip. J Pharm Biomed Anal. 2013;76:169-76.

23. Scott DA, Renaud DE, Krishnasamy S, Meriç P, Buduneli N, Cetinkalp S, et al. Diabetes-related molecular signatures in infrared spectra of human saliva. Diabetol Metab Syndr. 2010;2:48-.
24. Caixeta DC, Aguiar EMG, Cardoso-Sousa L, Coelho LMD, Oliveira SW, Espindola FS, et al. Salivary molecular spectroscopy: A sustainable, rapid and non-invasive monitoring tool for diabetes mellitus during insulin treatment. PLOS ONE. 2020;15(3):e0223461.
25. Singh AK, Mazumder AG, Halder P, Ghosh S, Chatterjee J, Roy A. Raman spectral probe and unique fractal signatures for human serum with diabetes and early stage diabetic retinopathy. Biomedical Physics & Engineering Express. 2018;5(1):015021.
26. Zhang Q, Kong X, Yuan H, Guan H, Li Y, Niu Y. Mangiferin Improved Palmitate-Induced-Insulin Resistance by Promoting Free Fatty Acid Metabolism in HepG2 and C2C12 Cells via PPARα: Mangiferin Improved Insulin Resistance. Journal of Diabetes Research. 2019;2019:2052675.
27. Liang G, Wang F, Song X, Zhang L, Qian Z, Jiang G. 3-Deoxyglucosone induces insulin resistance by impairing insulin signaling in HepG2 cells. Mol Med Rep. 2016;13(5):4506-12.
28. Mohammadpour Z, Sharifi L, Norouzzadeh M, Kalikias Y, Mahmoudi M. Hyperglycemia Induction in HepG2 Cell Line. International Journal of Health Studies. 2016;22:28-9.
29. Gaigneaux A, Goormaghtigh E. A new dimension for cell identification by FTIR spectroscopy: depth profiling in attenuated total reflection. Analyst. 2013;138(14):4070-5.
30. Kazarian S, Chan KLA. ATR-FTIR spectroscopic imaging: Recent advances and applications to biological systems. Analyst. 2013;138:1940-51.
31. Wehbe K, Filik J, Frogley MD, Cinque G. The effect of optical substrates on micro-FTIR analysis of single mammalian cells. Analytical and Bioanalytical Chemistry. 2013;405(4):1311-24.
32. Baker MJ, Trevisan J, Bassan P, Bhargava R, Butler HJ, Dorling KM, et al. Using Fourier transform IR spectroscopy to analyze biological materials. Nature protocols. 2014;9(8):1771-91.
33. Pedro L Fale AA, K L Andrew Chan. In situ Fourier transform infrared analysis of live cells' response to doxorubicin. Biochim Biophys Acta. 2015;Oct;1853((10 Pt A))::2640-8.
34. Altharawi A, Rahman KM, Chan KLA. Identifying the Responses from the Estrogen Receptor-Expressed MCF7 Cells Treated in Anticancer Drugs of Different Modes of Action Using Live-Cell FTIR Spectroscopy. ACS Omega. 2020;5(22):12698-706.
35. Altharawi A, Rahman KM, Chan KLA. Towards identifying the mode of action of drugs using live-cell FTIR spectroscopy. Analyst. 2019;144(8):2725-35.
36. Cho K, Cho D-H. Telmisartan increases hepatic glucose production via protein kinase C ζ-dependent insulin receptor substrate-1 phosphorylation in HepG2 cells and mouse liver. Yeungnam University Journal of Medicine. 2018;36.
37. Li Y, Zhu W, Li J, Liu M, Wei M. Resveratrol suppresses the STAT3 signaling pathway and inhibits proliferation of high glucose-exposed HepG2 cells partly through SIRT1. Oncology reports. 2013;30.
38. Chandrasekaran K, Swaminathan K, Chatterjee S, Dey A. Apoptosis in HepG2 cells exposed to high glucose. Toxicology in vitro : an international journal published in association with BIBRA. 2009;24:387-96.
39. Ferrannini E, Björkman O, Reichard G, Pilo A, Olsson M, Wahren J, et al. The Disposal of an Oral Glucose Load in Healthy Subjects: A Quantitative Study. Diabetes. 1985;34:580-8.
40. Han H-S, Kang G, Kim JS, Choi BH, Koo S-H. Regulation of glucose metabolism from a liver-centric perspective. Exp Mol Med. 2016;48(3):e218-e.
41. Adeva M, Pérez-Felpete N, Fernández-Fernández C, Donapetry-García C, Pazos-García C. Liver glucose metabolism in humans. Bioscience reports. 2016;36.
42. Poitout V, Robertson RP. Glucolipotoxicity: Fuel Excess and β-Cell Dysfunction. Endocrine Reviews. 2008;29(3):351-66.
43. Nakamura S, Takamura T, Matsuzawa-Nagata N, Takayama H, Misu H, Noda H, et al. Palmitate induces insulin resistance in H4IIEC3 hepatocytes through reactive oxygen species produced by mitochondria. J Biol Chem. 2009;284(22):14809-18.

44. García-Ruiz I, Solís-Muñoz P, Fernández-Moreira D, Muñoz-Yagüe T, Solís-Herruzo JA. In vitro treatment of HepG2 cells with saturated fatty acids reproduces mitochondrial dysfunction found in nonalcoholic steatohepatitis. Disease Models & Mechanisms. 2015;8(2):183.
45. Raza H, Prabu SM, Robin M-A, Avadhani N. Elevated Mitochondrial Cytochrome P450 2E1 and Glutathione S-Transferase A4-4 in Streptozotocin-Induced Diabetic Rats Tissue-Specific Variations and Roles in Oxidative Stress. Diabetes. 2004;53:185-94.
46. Alnahdi A, John A, Raza H. Augmentation of Glucotoxicity, Oxidative Stress, Apoptosis and Mitochondrial Dysfunction in HepG2 Cells by Palmitic Acid. Nutrients. 2019;11(9):1979.
47. Iyer VV, Yang H, Ierapetritou MG, Roth CM. Effects of glucose and insulin on HepG2-C3A cell metabolism. Biotechnology and Bioengineering. 2010;107(2):347-56.
48. Nagarajan S, Paul-Heng M, Krycer J, Fazakerley D, Sharland A, Hoy A. Lipid and Glucose Metabolism in Hepatocyte Cell Lines and Primary Mouse Hepatocytes: A comprehensive resource for in vitro studies of hepatic metabolism. American Journal of Physiology-Endocrinology and Metabolism. 2019;316.
49. Zheng J. Energy metabolism of cancer: Glycolysis versus oxidative phosphorylation (Review). Oncol Lett. 2012;4(6):1151-7.
50. Warburg O. On the Origin of Cancer Cells. Science. 1956;123(3191):309.
51. Wiercigroch E, Szafraniec E, Czamara K, Pacia MZ, Majzner K, Kochan K, et al. Raman and infrared spectroscopy of carbohydrates: A review. Spectrochimica Acta Part A: Molecular and Biomolecular Spectroscopy. 2017;185:317-35.
52. Geciova J, Bury D, Jelen P. Methods for disruption of microbial cells for potential use in the dairy industry--a review. Int Dairy J. 2002;12(6):541-53.
53. Csepregi R, Temesfői V, Sali N, Poór M, W Needs P, A Kroon P, et al. A One-Step Extraction and Luminescence Assay for Quantifying Glucose and ATP Levels in Cultured HepG2 Cells. Int J Mol Sci. 2018;19(9):2670.